Journal of Mathematical Modeling
Vol. 14, No. 3, 2026, pp. 1071-1091. Research Article

JMM

An investigation on transmission and control of fractional-order hepatitis B model

Deepak[†], Lokesh Kumar Yadav[†], Murli Manohar Gour[†], Sunil Dutt Purohit[§*]

[†]*Department of Mathematics, Vivekananda Global University Jaipur, India*
[§]*Department of HEAS(Mathematics), Rajasthan Technical University, Kota, Rajasthan, India*

Email(s): deepak@vgu.ac.in, lokesh.yadav@vgu.ac.in, murlimanohar.gaur@vgu.ac.in, sunil_a_purohit@yahoo.com

Abstract. Mathematical models are useful for understanding and managing infectious diseases. They assist researchers and public health personnel in decision-making by providing data, evaluating the impact of interventions, and estimating the spread of diseases. The main objective of the present work is to provide an in-depth analysis of the transmission and control of a hepatitis B model under the Caputo fractional derivative, including both qualitative and semi-analytical investigations. Fixed-point theory is employed to establish the conditions for the existence and uniqueness of solutions to the proposed model. The obtained solutions are graphically simulated using MATLAB. The physical significance of this study lies in its ability to capture memory effects and long-term dependencies in the transmission dynamics of the hepatitis B model, which cannot be explained by classical models. The results provide valuable insights for designing effective disease-control strategies and contribute to the advancement of fractional epidemiological modeling, with potential applications in public health policy and clinical research.

Keywords: Fractional hepatitis B virus model, Caputo fractional derivative, existence theory, fixed point theory, semi analytical results.
AMS Subject Classification 2010: 26A33, 34A08, 93A30.

1 Introduction

Hepatitis B is a dangerous disease caused by the hepatitis virus. It is a significant global health problem. This disease leads to serious chronic liver infections, putting people's lives at high risk. Hepatitis B is also a primary cause of liver cancer [48]. The infection occurs when the virus enters the bloodstream and reaches the liver, where it causes damage [33].

*Corresponding author
Received: 05 October 2025/ Revised: 28 February 2026/ Accepted: 11 April 2026
DOI: 10.22124/jmm.2026.31885.2878

Hepatitis B has two stages: an acute stage lasting up to six months, which is often cleared by the immune system, and a chronic stage that lasts longer than six months. Both adults and children can contract this infection. Hepatitis B virus (HBV) is a serious disease that can be transmitted from an infected individual to a healthy person, making the affected individuals chronic carriers. Nearly 240 million people worldwide have chronic liver infections, and approximately 6,00,000 people die each year due to this dangerous disease.

Mathematical modeling facilitates precise definition and analysis of real-world events by employing various mathematical approaches, including fractional calculus [13, 19]. Its significance has grown notably within mathematical science, allowing us to transform real-world issues into equations, mathematical language, and then use appropriate approaches to predict results. Modeling has a wide range of applications, serving as a tool for anticipating or estimating future ramifications, making it an essential approach in many different fields [5, 23, 32, 35, 39, 43, 44]. Recently, researchers have used the tools of fractional calculus for modeling various dynamical phenomena across nearly all disciplines of applied sciences, as these describe dynamic behaviors more precisely compared to natural-order derivatives [3,31,49]. Researchers have introduced a variety of concepts for fractional derivatives, with notable ones being the Riemann–Liouville, Caputo, and Hadamard derivatives [29, 30, 38, 41, 50–52]. These derivatives have been extensively studied from many perspectives, including approximate solutions, stability, existence, and uniqueness of numerous biological and physical models [4, 21, 26].

Mathematical modeling is a key approach to understand the transmission dynamics of infectious diseases, including HBV. Many studies have investigated the transmission and control of HBV [6, 36, 37, 45, 47, 54]. Kamyad et al. [24] formulated an integer-order compartmental model for HBV transmission, incorporating susceptible (S), exposed (E), acutely infected (I), chronic carrier (C), and recovered (R) classes, with parameters for birth/death rates, infection rates, and recovery transitions. The governing system of ordinary differential equations is given by:

$$\begin{cases} \frac{dS(\xi)}{d\xi} = \vartheta - [\vartheta q_1 C + \vartheta q_2 R + q'(I+\mu C)S + \vartheta S + \rho_1 S] + \kappa_4 R, \\ \frac{dE(\xi)}{d\xi} = q'(I+\mu C)S - (\vartheta+\kappa_1)E, \\ \frac{dI(\xi)}{d\xi} = \kappa_1 E - (\vartheta+\kappa_2)I, \\ \frac{dC(\xi)}{d\xi} = [\vartheta q_1 - (\vartheta+\kappa_3-\rho_2)]C + q_3\kappa_2 I, \\ \frac{dR(\xi)}{d\xi} = (\vartheta q_2 - \vartheta - \kappa_4)R + (1-q_3)\kappa_2 I + (\kappa_3+\rho_2)C + \rho_1 S. \end{cases} \tag{1}$$

In the given model, $S(\xi)$ stands for the density of susceptible individuals, $E(\xi)$ for exposed individuals, $I(\xi)$ for infected individuals, $C(\xi)$ for chronic HBV carriers, and $R(\xi)$ for recovered individuals. In this model, ϑ represents the per capita birth and death rate, while κ_1, κ_2, and κ_3 denote the rates at which individuals become exposed, transition to carrier status, and move from carrier to recovered, respectively. Additionally, μ is the infectiousness rate of carriers relative to acute infections, and q_3 is the proportion of acutely infected individuals who become carriers.

According to the law of mass action, the infection transmits horizontally at a rate of $q'(I+\mu C)S$, where q' is the contact rate. The infection also transmits vertically at a rate of p_1 among newborns, represented by the term $\vartheta q_1 C$, where $q_1 < 1$. Furthermore, q_2 of newborns from the recovered class are immune, expressed by $\vartheta q_2 R$, where $q_2 < 1$.

Kamyad et al. [24] investigated a mathematical model (1) for the transmission dynamics and optimal control of HBV vaccine and therapy, and provided a graphical solution. Khan et al. [27] converted model

(1) into a fractional order model involving the Caputo-Fabrizio derivative operator, and using a semi-analytic technique, namely, the Laplace-Adomian decomposition method, presented the graphical nature of the proposed model. Recently, Gour et al. [15] investigated a fractionalized model for HBV infection, focusing on curing infected cells, and analyzed that the peak of viral propagation is reduced and cell damage is minimized by initiating treatment at an early stage.

In the present study, our objective is to obtain analytical and graphical solutions for the proposed HBV model using the homotopy decomposition method (HDM) [9], while analyzing the system in fractional and integer orders. The HDM is a relatively recent semi-analytical technique for solving systems of fractional partial differential equations. Unlike conventional methods, it avoids restrictive assumptions and discretization, reduces computational complexity, and naturally incorporates non-local effects. The physical and clinical significance of this work lies in its enhanced ability to capture memory effects and relapse phenomena more realistically than classical approaches, thereby providing deeper insights into the long-term behavior of HBV infection. These findings are not only mathematically meaningful but also highly relevant to healthcare systems, as they can inform treatment optimization, vaccination strategies, and public health interventions aimed at reducing the global burden of HBV.

The novelty of this study resides in the integration of the Caputo fractional framework with the HDM to simultaneously analyze both acute and chronic phases of HBV dynamics. While many existing studies focus either on integer-order models or on fractional models limited to a single infection stage, our approach unifies vaccination, treatment effects, memory phenomena, and relapse behavior within a single coherent system. Furthermore, in contrast to works that rely predominantly on purely numerical schemes, we obtain semi-analytical approximations through HDM, which are validated by numerical simulations. This dual analytical-numerical perspective provides a more thorough theoretical knowledge while also providing therapeutically useful insights for long-term illness control and prevention methods. The Caputo fractional derivative is especially useful here because it preserves the physical interpretability of standard initial conditions while effectively accounting for memory and hereditary effects in HBV transmission, such as delayed immune responses and persistent viral carriage, which integer-order models cannot capture.

The remainder of this paper is organized as follows. Section 2 presents the fundamental definitions of fractional calculus and introduces the fractional-order HBV model. Section 3 describes the basic idea of the proposed technique. Section 4 provides a qualitative analysis of the model, including existence, uniqueness, and stability of the solution. In Section 5, we implement the HDM to compute the fractional model. Section 6 presents numerical simulations using MATLAB and available data to validate the analytical results and summarize the findings. Finally, Section 7 concludes the paper. References are given at the end of the paper.

2 Fractional calculus

Fractional calculus stands as a prized asset within mathematics, offering exceptional significance in the realm of mathematical modeling. Its capacity to characterize natural phenomena surpasses that of classical calculus, providing more precise descriptions. Moreover, it proves highly advantageous for delineating nonlinear phenomena across various scientific and technological domains. Currently, numerous scholars harness this potent tool, enhancing the quality and depth of their research endeavors. In medical science, fractional calculus finds extensive application in the study of fractional-order disease

models, like Coronavirus dynamics [7, 11, 14, 20, 22, 25, 28], HIV [53], Chikungunya virus [8], influenza disease [10], HBV [2, 18, 34, 40, 42, 46] and other disease models [1, 12, 16, 17].

2.1 The fractional-order HBV model

To capture memory effects, long-term dependencies and hereditary properties inherent in the dynamics of HBV transmission, such as delayed immune responses and persistent viral carriage, we extend the integer-order model (1) from Kamyad et al. [24] by replacing ordinary derivatives with Caputo fractional derivatives of order $\varsigma \in (0,1]$.

The resulting governing system of fractional differential equations, the central model of this work, is given by

$$
\begin{aligned}
{}^{C}D_{\xi}^{\varsigma} S(\xi) &= \vartheta - \left[\vartheta q_1 C + \vartheta q_2 R + q'(I+\mu C)S + \vartheta S + \rho_1 S\right] + \kappa_4 R, && (2)\\
{}^{C}D_{\xi}^{\varsigma} E(\xi) &= q'(I+\mu C)S - (\vartheta+\kappa_1)E, && (3)\\
{}^{C}D_{\xi}^{\varsigma} I(\xi) &= \kappa_1 E - (\vartheta+\kappa_2)I, && (4)\\
{}^{C}D_{\xi}^{\varsigma} C(\xi) &= \left[\vartheta q_1 - (\vartheta+\kappa_3-\rho_2)\right]C + q_3\kappa_2 I, && (5)\\
{}^{C}D_{\xi}^{\varsigma} R(\xi) &= (\vartheta q_2 - \vartheta - \kappa_4)R + (1-q_3)\kappa_2 I + (\kappa_3+\rho_2)C + \rho_1 S, && (6)
\end{aligned}
$$

where $0 < \varsigma \leq 1$, and the state variables (S, E, I, C, R) and parameters are defined as in the integer-order model (1). with the initial conditions

$$
\begin{aligned}
S(0) &= S_0, && (7)\\
E(0) &= E_0, && (8)\\
I(0) &= I_0, && (9)\\
C(0) &= C_0, && (10)\\
R(0) &= R_0. && (11)
\end{aligned}
$$

This Caputo-based formulation is particularly suitable for HBV epidemiology, as it preserves standard initial conditions while effectively incorporating non-local and memory-dependent behaviors that classical integer-order models cannot adequately capture.

2.2 Basic Definitions

Definition 1. *The Riemann-Liouville fractional derivative of $\varkappa$ of order $\varsigma > 0$ is defined as follows*

$$
{}_{a}^{RL}D_{\xi}^{\varsigma}\varkappa(\xi) = \frac{1}{\Gamma(q-\varsigma)}\frac{d^q}{d\xi^q}\int_a^{\xi}(\xi-\Psi)^{q-\varsigma-1}\varkappa(\Psi)\,d\Psi,\ \xi>0,\ q-1<\varsigma\leq q,\ q\in Z^{+}. \qquad (12)
$$

Definition 2. *Let $\upsilon \in \mathbb{R}$. A real-valued function $\varkappa(\xi)$, $\xi > 0$, is said to belong to the space C_{υ} if there exists a real number $K > \upsilon$ such that*

$$
\varkappa(\xi) = \xi^{K}\varkappa_1(\xi),
$$

where $\varkappa_1(\xi) \in C[0,\infty)$. The function $\varkappa$ is said to belong to the space C_{υ}^{σ} ($\sigma \in \mathbb{N}$) if its σ-th derivative satisfies $\varkappa^{(\sigma)} \in C_{\upsilon}$.

Definition 3. *The Caputo fractional derivative of $\varkappa$ of order $\varsigma > 0$ is defined as follows*

$$ {}_{a}^{C}D_{\xi}^{\varsigma}\varkappa(\xi) = \frac{1}{\Gamma(q-\varsigma)}\int_{a}^{\xi}(\xi-\Psi)^{q-\varsigma-1}\varkappa'(\Psi)\,d\Psi,\ \xi>0, q-1<\varsigma\le q,\ q\in Z^{+}. \tag{13} $$

In addition, the corresponding fractional integral of order ς, with $\Re(\varsigma)>0$ is given by

$$ \Im^{\varsigma}[\varkappa(\xi)] = \frac{1}{\Gamma(\varsigma)}\int_{0}^{\xi}(\xi-\Psi)^{\varsigma-1}\varkappa(\Psi)d\Psi,\ \ \varsigma>0,\ \xi>0, \tag{14} $$

and

$$ \Im^{0}[\varkappa(\xi)] = \varkappa(\xi). \tag{15} $$

3 Proposed methodology

The HDM is a powerful semi-analytical technique for obtaining series solutions to nonlinear fractional differential equations. It constructs a continuous deformation (homotopy) between an initial simple problem and the target complex problem, leading to a series expansion in powers of an embedding parameter $p \in [0,1]$. Consider a fractional-order non-homogeneous differential equation as [9]

$$ D_{\xi}^{\varsigma}[\varkappa(\xi)] = \Re[\varkappa(\xi)] + \aleph[\varkappa(\xi)] + h(\xi),\ \ 0<\varsigma\le 1, \tag{16} $$

accompanied by the initial condition

$$ \varkappa(\xi_0) = \varphi, \tag{17} $$

where, D_{ξ}^{ς} denotes Caputo derivative with fractional order ς, and $\Re$ & $\aleph$ represent linear & nonlinear functions respectively, while h is source term.
First, we reduce equation (16) into following form

$$ \varkappa(\xi) - \varkappa(0) = \frac{1}{\Gamma\varsigma}\int_{0}^{\xi}(\xi-\mu)^{\varsigma-1}[\Re[\varkappa(\mu)] + \aleph[\varkappa(\mu)] + h(\mu)]\,d\mu. \tag{18} $$

In the proposed method, the fundamental assumption is that the solution can be expressed as a power series in the embedding parameter p

$$ \varkappa(\xi,p) = \sum_{\rho=0}^{\infty} p^{\rho}\varkappa_{\rho}(\xi), \tag{19} $$

and

$$ \varkappa(\xi) = \lim_{p\to 1}\varkappa(\xi,p). \tag{20} $$

The nonlinear term $\aleph[\varkappa(\xi)]$ is decomposed as

$$ \aleph[\varkappa(\xi)] = \sum_{\rho=0}^{\infty} p^{\rho}\mathscr{H}_{\rho}(\varkappa), \tag{21} $$

where, $p \in (0,1]$ is the embedding parameter. Here, $\mathscr{H}_\rho(\varkappa)$ signifies He's polynomial, which can be stated as

$$\mathscr{H}_\rho\left(\varkappa_0,\varkappa_1,\varkappa_2,...,\varkappa_\rho\right)=\frac{1}{\Gamma(\rho+1)}\frac{\partial^\rho}{\partial p^\rho}\left[\aleph\left(\sum_{k=0}^{\infty}p^k\varkappa_k(\xi)\right)\right]. \tag{22}$$

By substituting equations (19), (21), and (22) into equation (18), we obtain

$$\begin{aligned}&\sum_{\rho=0}^{\infty}p^\rho\varkappa_\rho(\xi)-\varkappa(0)\\&\quad=p\left(\tfrac{1}{\Gamma\varsigma}\int_0^\xi(\xi-\mu)^{\varsigma-1}\left[\Re\left[\sum_{\rho=0}^{\infty}p^\rho\varkappa_\rho(\mu)\right]+\aleph\left[\sum_{\rho=0}^{\infty}p^\rho\varkappa_\rho(\mu)\right]+h(\mu)\right]d\mu\right).\end{aligned} \tag{23}$$

By comparing identical powers of p on both sides, we obtain solutions of various orders, beginning with an initial approximation

$$\varkappa_0(\xi)=\varphi. \tag{24}$$

Thus, the solution of equation (16) is given as

$$\varkappa=\varkappa_0+\varkappa_1+\varkappa_2+\cdots+\varkappa_\rho. \tag{25}$$

4 Existence and uniqueness

Theorem 1. *Let $\Phi_1,\Phi_2,\Phi_3,\Phi_4$, and Φ_5 denote the nonlinear kernels of the proposed fractional model corresponding to the unknown variables $S(\xi),E(\xi),I(\xi),C(\xi),R(\xi)$, respectively. Then the Caputo fractional system (2)–(6) is equivalent to a system of nonlinear Volterra integral equations.*

Proof. Applying the Caputo fractional integral operator of order ς to both sides of equations (2)–(6) and using the initial conditions, we obtain

$$S(\xi)=S(0)+\frac{1}{\Gamma(\varsigma)}\int_0^\xi(\xi-\varkappa)^{\varsigma-1}\Phi_1(S,E,I,C,R;\varkappa)\,d\varkappa, \tag{26}$$

$$E(\xi)=E(0)+\frac{1}{\Gamma(\varsigma)}\int_0^\xi(\xi-\varkappa)^{\varsigma-1}\Phi_2(S,E,I,C,R;\varkappa)\,d\varkappa, \tag{27}$$

$$I(\xi)=I(0)+\frac{1}{\Gamma(\varsigma)}\int_0^\xi(\xi-\varkappa)^{\varsigma-1}\Phi_3(S,E,I,C,R;\varkappa)\,d\varkappa, \tag{28}$$

$$C(\xi)=C(0)+\frac{1}{\Gamma(\varsigma)}\int_0^\xi(\xi-\varkappa)^{\varsigma-1}\Phi_4(S,E,I,C,R;\varkappa)\,d\varkappa, \tag{29}$$

$$R(\xi)=R(0)+\frac{1}{\Gamma(\varsigma)}\int_0^\xi(\xi-\varkappa)^{\varsigma-1}\Phi_5(S,E,I,C,R;\varkappa)\,d\varkappa. \tag{30}$$

Here, we have the following kernels

$$\Phi_1=\vartheta-\left[\vartheta q_1C+\vartheta q_2R+q'(I+\mu C)S+\vartheta S+\rho_1S\right]+\kappa_4R, \tag{31}$$

$$\Phi_2 = q'(I+\mu C)S-(\vartheta+\kappa_1)E, \tag{32}$$
$$\Phi_3 = \kappa_1 E-(\vartheta+\kappa_2)I, \tag{33}$$
$$\Phi_4 = [\vartheta q_1-(\vartheta+\kappa_3-\rho_2)]C+q_3\kappa_2 I, \tag{34}$$
$$\Phi_5 = (\vartheta q_2-\vartheta-\kappa_4)R+(1-q_3)\kappa_2 I+(\kappa_3+\rho_2)C+\rho_1 S. \tag{35}$$

Hence, the Caputo fractional differential system is transformed into an equivalent nonlinear Volterra integral system. □

Theorem 2. *The kernels* Φ_1, Φ_2, Φ_3, Φ_4, *and* Φ_5 *satisfy the Lipschitz's condition.*

Proof. First, we demonstrate that Φ_1 satisfies the Lipschitz condition. Let S and $\tilde{S}$ be two functions, then

$$\begin{aligned}\left\|\Phi_1(\xi,S)-\Phi_1\left(\xi,\tilde{S}\right)\right\| = \Big\|\big(\vartheta-\big[\vartheta q_1 C(\xi)+\vartheta q_2 R(\xi)+q'(I+\mu C(\xi))S(\xi)+\vartheta S(\xi)\\ +\rho_1 S(\xi)\big]+\kappa_4 R(\xi)\big)-\big(\vartheta-\big[\vartheta q_1 C(\xi)+\vartheta q_2 R(\xi)+q'\\ \times(I+\mu C(\xi))\tilde{S}(\xi)+\vartheta\tilde{S}(\xi)+\rho_1\tilde{S}(\xi)\big]+\kappa_4 R(\xi)\big)\Big\|.\end{aligned} \tag{36}$$

Using Cauchy's inequality, we have

$$\left\|\Phi_1(\xi,S)-\Phi_1\left(\xi,\tilde{S}\right)\right\| \le \left\|q'(I+\mu C(\xi))+\vartheta+\rho_1\right\|\left\|S(\xi)-\tilde{S}(\xi)\right\|, \tag{37}$$

or

$$\left\|\Phi_1(\xi,S)-\Phi_1\left(\xi,\tilde{S}\right)\right\| \le \Theta_1\left\|S(\xi)-\tilde{S}(\xi)\right\|, \tag{38}$$

where

$$\left\|q'(I+\mu C(\xi))+\vartheta+\rho_1\right\| \le \Theta_1\,. \tag{39}$$

For Φ_2

$$\begin{aligned}\left\|\Phi_2(\xi,E)-\Phi_2\left(\xi,\tilde{E}\right)\right\| = \Big\|\big(q'(I+\mu C(\xi))S(\xi)-(\vartheta+\kappa_1)E(\xi)\big)\\ -\big(q'(I+\mu C(\xi))S(\xi)-(\vartheta+\kappa_1)\tilde{E}(\xi)\big)\Big\|,\end{aligned} \tag{40}$$

and by using Cauchy's inequality, we have

$$\left\|\Phi_2(\xi,E)-\Phi_2\left(\xi,\tilde{E}\right)\right\| \le \|(\vartheta+\kappa_1)\|\left\|E(\xi)-\tilde{E}(\xi)\right\|, \tag{41}$$

or

$$\left\|\Phi_2(\xi,E)-\Phi_2\left(\xi,\tilde{E}\right)\right\| \le \Theta_2\left\|E(\xi)-\tilde{E}(\xi)\right\|, \tag{42}$$

where

$$\|(\vartheta+\kappa_1)\| \le \Theta_2\,. \tag{43}$$

For Φ_3

$$\left\|\Phi_3(\xi,I)-\Phi_3\left(\xi,\tilde{I}\right)\right\| = \|(\kappa_1 E(\xi)-(\vartheta+\kappa_2)I(\xi))-\left(\kappa_1 E(\xi)-(\vartheta+\kappa_2)\tilde{I}(\xi)\right)\|, \tag{44}$$

and by using Cauchy's inequality, we have

$$\left\|\Phi_3(\xi,I)-\Phi_3\left(\xi,\tilde{I}\right)\right\| \le \|(\vartheta+\kappa_2)\|\left\|I(\xi)-\tilde{I}(\xi)\right\|, \tag{45}$$

or

$$\left\|\Phi_3(\xi,E)-\Phi_3\left(\xi,\tilde{E}\right)\right\| \leq \Theta_3\left\|I(\xi)-\tilde{I}(\xi)\right\|, \tag{46}$$

where

$$\|(\vartheta+\kappa_2)\| \leq \Theta_3\,. \tag{47}$$

For Φ_4

$$\begin{aligned}\left\|\Phi_4(\xi,C)-\Phi_4\left(\xi,\tilde{C}\right)\right\| = \|(\{\vartheta q_1-(\vartheta+\kappa_3-\rho_2)\}C(\xi)+q_3\kappa_2 I(\xi))\\ -\left(\{\vartheta q_1-(\vartheta+\kappa_3-\rho_2)\}\tilde{C}(\xi)+q_3\kappa_2 I(\xi)\right)\|,\end{aligned} \tag{48}$$

and by using Cauchy's inequality, we have

$$\left\|\Phi_4(\xi,C)-\Phi_4\left(\xi,\tilde{C}\right)\right\| \leq \|(\vartheta+\kappa_3-\rho_2)\|\left\|C(\xi)-\tilde{C}(\xi)\right\|, \tag{49}$$

or

$$\left\|\Phi_4(\xi,C)-\Phi_4\left(\xi,\tilde{C}\right)\right\| \leq \Theta_4\left\|C(\xi)-\tilde{C}(\xi)\right\|, \tag{50}$$

where

$$\|(\vartheta+\kappa_3-\rho_2)\| \leq \Theta_4\,. \tag{51}$$

Finally, for Φ_5

$$\begin{aligned}\left\|\Phi_5(\xi,R)-\Phi_5\left(\xi,\tilde{R}\right)\right\| = \|((\vartheta q_2-\vartheta-\kappa_4)R(\xi)+(1-q_3)\kappa_2 I(\xi)+(\kappa_3+\rho_2)\\ \times C(\xi)+\rho_1 S(\xi))-\left((\vartheta q_2-\vartheta-\kappa_4)\tilde{R}(\xi)+(1-q_3)\kappa_2 I(\xi)\right.\\ \left.+(\kappa_3+\rho_2)C(\xi)+\rho_1 S(\xi)\right)\|,\end{aligned} \tag{52}$$

and by using Cauchy's inequality, we have

$$\left\|\Phi_5(\xi,R)-\Phi_5\left(\xi,\tilde{R}\right)\right\| \leq \|(\vartheta q_2-\vartheta-\kappa_4)\|\left\|R(\xi)-\tilde{R}(\xi)\right\|, \tag{53}$$

or

$$\left\|\Phi_5(\xi,R)-\Phi_5\left(\xi,\tilde{R}\right)\right\| \leq \Theta_5\left\|R(\xi)-\tilde{R}(\xi)\right\|, \tag{54}$$

where

$$\|(\vartheta q_2-\vartheta-\kappa_4)\| \leq \Theta_5\,. \tag{55}$$

Hence, the Lipschitz condition holds, and from equation (26) we obtain the following recursive formula

$$S_\ell(\xi)=\Phi_1(\xi,S_{\ell-1})+\frac{1}{\Gamma\varsigma}\int_0^\xi(\xi-\varkappa)^{\varsigma-1}\Phi_1(\varkappa,S_{\ell-1})\,d\varkappa. \tag{56}$$

So, the difference between two consecutive terms is given by

$$\begin{aligned}U_\ell(\xi)=S_\ell(\xi)-S_{\ell-1}(\xi)=\Phi_1(\xi,S_{\ell-1})-\Phi_1(\xi,S_{\ell-2})\\ +\tfrac{1}{\Gamma\varsigma}\int_0^\xi(\xi-\varkappa)^{\varsigma-1}\left(\Phi_1(\varkappa,S_{\ell-1})-\Phi_1(\varkappa,S_{\ell-2})\right)d\varkappa.\end{aligned} \tag{57}$$

By taking the norm of equation (57), we obtain

$$\begin{aligned}\|U_\ell(\xi)\| &= \|S_\ell(\xi) - S_{\ell-1}(\xi)\| \\ &= \Big\| \Phi_1\left(\xi, S_{\ell-1}\right) - \Phi_1\left(\xi, S_{\ell-2}\right) \\ &\quad + \frac{1}{\Gamma(\varsigma)} \int_0^\xi (\xi-\varkappa)^{\varsigma-1} \left[\Phi_1(\varkappa, S_{\ell-1}) - \Phi_1(\varkappa, S_{\ell-2})\right] d\varkappa \Big\| \\ &\leq \|\Phi_1(\xi, S_{\ell-1}) - \Phi_1(\xi, S_{\ell-2})\| \\ &\quad + \frac{1}{\Gamma(\varsigma)} \int_0^\xi (\xi-\varkappa)^{\varsigma-1} \|\Phi_1(\varkappa, S_{\ell-1}) - \Phi_1(\varkappa, S_{\ell-2})\| \, d\varkappa. \end{aligned} \tag{58}$$

Similarly using equations (27)-(30), we obtain

$$\begin{aligned}\|V_\ell(\xi)\| &= \|E_\ell(\xi) - E_{\ell-1}(\xi)\| \\ &\leq \|\Phi_2(\xi, E_{\ell-1}) - \Phi_2(\xi, E_{\ell-2})\| \\ &\quad + \frac{1}{\Gamma\varsigma} \int_0^\xi \Big\| (\xi-\varkappa)^{\varsigma-1} \left(\Phi_2(\varkappa, E_{\ell-1}) - \Phi_2(\varkappa, E_{\ell-2})\right) \Big\| \, d\varkappa. \end{aligned} \tag{59}$$

$$\begin{aligned}\|W_\ell(\xi)\| &= \|I_\ell(\xi) - I_{\ell-1}(\xi)\| \\ &\leq \|\Phi_3(\xi, I_{\ell-1}) - \Phi_3(\xi, I_{\ell-2})\| \\ &\quad + \frac{1}{\Gamma\varsigma} \int_0^\xi \Big\| (\xi-\varkappa)^{\varsigma-1} \left(\Phi_3(\varkappa, I_{\ell-1}) - \Phi_3(\varkappa, I_{\ell-2})\right) \Big\| \, d\varkappa. \end{aligned} \tag{60}$$

$$\begin{aligned}\|\chi_\ell(\xi)\| &= \|C_\ell(\xi) - C_{\ell-1}(\xi)\| \\ &\leq \|\Phi_4(\xi, C_{\ell-1}) - \Phi_4(\xi, C_{\ell-2})\| \\ &\quad + \frac{1}{\Gamma\varsigma} \int_0^\xi \Big\| (\xi-\varkappa)^{\varsigma-1} \left(\Phi_4(\varkappa, C_{\ell-1}) - \Phi_4(\varkappa, C_{\ell-2})\right) \Big\| \, d\varkappa. \end{aligned} \tag{61}$$

$$\begin{aligned}\|Z_\ell(\xi)\| &= \|R_\ell(\xi) - R_{\ell-1}(\xi)\| \\ &\leq \|\Phi_5(\xi, R_{\ell-1}) - \Phi_5(\xi, R_{\ell-2})\| \\ &\quad + \frac{1}{\Gamma\varsigma} \int_0^\xi \Big\| (\xi-\varkappa)^{\varsigma-1} \left(\Phi_5(\varkappa, R_{\ell-1}) - \Phi_5(\varkappa, R_{\ell-2})\right) \Big\| \, d\varkappa. \end{aligned} \tag{62}$$

□

Theorem 3. *The considered HBV model has a solution under the restriction* $\Im_1 + J_1(\xi_0)^\varsigma < 1, \Im_2 + J_2(\xi_0)^\varsigma < 1, \Im_3 + J_3(\xi_0)^\varsigma < 1, \Im_4 + J_4(\xi_0)^\varsigma < 1,$ *and* $\Im_5 + J_5(\xi_0)^\varsigma < 1.$

Proof. Since S, E, I, C, and R are bounded functions and equation (57) holds, (58) implies that

$$\|U_\ell(\xi)\| \leq \|S(0)\| \left\{\Im_1 + J_1(\xi_0)^\varsigma\right\}^\ell. \tag{63}$$

Moreover, the kernels Φ_1, Φ_2, Φ_3, Φ_4, and Φ_5 satisfy the Lipschitz conditions. Therefore, the recursive relation (58) can be expressed as

$$S(\xi) - S(0) = S_\ell(\xi) - \wp_\ell(\xi). \tag{64}$$

Hence, we obtain

$$\|\wp_\ell(\xi)\| = \left\| (\Phi_1(\xi, S) - \Phi_1(\xi, S_{\ell-1})) + \frac{1}{\Gamma(\varsigma)} \int_0^\xi (\xi - \varkappa)^{\varsigma-1} (\Phi_1(\varkappa, S) - \Phi_1(\varkappa, S_{\ell-1}))\, d\varkappa \right\|. \tag{65}$$

Using the triangle inequality, we get

$$\begin{aligned} \|\wp_\ell(\xi)\| \leq{}& \|\Phi_1(\xi, S) - \Phi_1(\xi, S_{\ell-1})\| \\ &+ \frac{1}{\Gamma(\varsigma)} \left\| \int_0^\xi (\xi - \varkappa)^{\varsigma-1} (\Phi_1(\varkappa, S) - \Phi_1(\varkappa, S_{\ell-1}))\, d\varkappa \right\|. \end{aligned} \tag{66}$$

Applying the Lipschitz property of Φ_1, it follows that

$$\|\wp_\ell(\xi)\| \leq \Im \|S - S_{\ell-1}\| + \xi^\varsigma J \|S - S_{\ell-1}\|. \tag{67}$$

Solving recursively, we obtain

$$\|\wp_\ell(\xi)\| \leq \{\Im_1 + J_1 \xi^\varsigma\}^{\ell+1} \Psi. \tag{68}$$

Evaluating at $\xi = \xi_0$, we obtain

$$\|\wp_\ell(\xi_0)\| \leq \left\{\Im_1 + J_1 \xi_0^\varsigma\right\}^{\ell+1} \Psi. \tag{69}$$

Finally, taking the limit as $\ell \to \infty$, we obtain

$$\|\wp_\ell(\xi)\| \to 0. \tag{70}$$

Thus, the existence is established. Other results can be proved in a similar manner. □

Theorem 4. *The considered HBV model has a unique solution.*

Proof. To demonstrate the uniqueness, we suppose that there is an another set of solutions for the system (2)-(6), which are provided by $S_1(\xi)$, $E_1(\xi)$, $I_1(\xi)$, $C_1(\xi)$, and $R_1(\xi)$. Firstly, we consider

$$\begin{aligned} S(\xi) - S_1(\xi) = {}& (\Phi_1(\xi, S) - \Phi_1(\xi, S_1)) \\ &+ \frac{1}{\Gamma\varsigma} \int_0^\xi (\xi - \varkappa)^{\varsigma-1} (\Phi_1(\varkappa, S) - \Phi_1(\varkappa, S_1))\, d\varkappa. \end{aligned} \tag{71}$$

Taking the norm of equation (71), we obtain

$$\|S(\xi) - S_1(\xi)\| \leq \|(\Phi_1(\xi, S) - \Phi_1(\xi, S_1))\|$$

$$+\frac{1}{\Gamma\varsigma}\int_0^{\xi}\left\|\left\{(\xi-\varkappa)^{\varsigma-1}\left(\Phi_1(\varkappa,S)-\Phi_1(\varkappa,S_1)\right)\right\}\right\|d\varkappa. \tag{72}$$

Since the kernel Φ_1 satisfies the Lipschitz condition and the solution is bounded, it follows that $\|S(\xi)-S_1(\xi)\|=0$. Therefore, $S(\xi)=S_1(\xi)$.

By applying the same argument to the remaining equations, we obtain

$$E(\xi)=E_1(\xi),\qquad I(\xi)=I_1(\xi),\qquad C(\xi)=C_1(\xi),\qquad R(\xi)=R_1(\xi).$$

Thus, the solution of the HBV system is unique. □

5 Approximate solution of proposed model

Based on the proposed strategy, we get

$$\begin{aligned}\sum_{\ell=0}^{\infty}P^{\ell}S_{\ell}(\xi)&=S(0)+\frac{p}{\Gamma\varsigma}\int_0^{\xi}(\xi-\varkappa)^{\varsigma-1}\left[\vartheta-\vartheta q_1\left(\sum_{\ell=0}^{\infty}P^{\ell}C_{\ell}(\varkappa)\right)-\vartheta q_2\left(\sum_{\ell=0}^{\infty}P^{\ell}R_{\ell}(\varkappa)\right)\right.\\&\quad-q'\left(\sum_{\ell=0}^{\infty}P^{\ell}I_{\ell}(\varkappa)\sum_{\ell=0}^{\infty}P^{\ell}S_{\ell}(\varkappa)\right)-q'\mu\left(\sum_{\ell=0}^{\infty}P^{\ell}C_{\ell}(\varkappa)\sum_{\ell=0}^{\infty}P^{\ell}S_{\ell}(\varkappa)\right)\\&\quad\left.-\vartheta\left(\sum_{\ell=0}^{\infty}P^{\ell}S_{\ell}(\varkappa)\right)-\rho_1\left(\sum_{\ell=0}^{\infty}P^{\ell}S_{\ell}(\varkappa)\right)+\kappa_4\left(\sum_{\ell=0}^{\infty}P^{\ell}R_{\ell}(\varkappa)\right)\right]d\varkappa,\end{aligned} \tag{73}$$

$$\begin{aligned}\sum_{\ell=0}^{\infty}P^{\ell}E_{\ell}(\xi)&=E(0)+\frac{p}{\Gamma\varsigma}\int_0^{\xi}(\xi-\varkappa)^{\varsigma-1}\left[q'\left(\sum_{\ell=0}^{\infty}P^{\ell}I_{\ell}(\varkappa)\sum_{\ell=0}^{\infty}P^{\ell}S_{\ell}(\varkappa)\right)\right.\\&\quad\left.+q'\mu\left(\sum_{\ell=0}^{\infty}P^{\ell}C_{\ell}(\varkappa)\sum_{\ell=0}^{\infty}P^{\ell}S_{\ell}(\varkappa)\right)-(\vartheta+\kappa_1)\left(\sum_{\ell=0}^{\infty}P^{\ell}E_{\ell}(\varkappa)\right)\right]d\varkappa,\end{aligned} \tag{74}$$

$$\sum_{\ell=0}^{\infty}P^{\ell}I_{\ell}(\xi)=I(0)+\frac{p}{\Gamma\varsigma}\int_0^{\xi}(\xi-\varkappa)^{\varsigma-1}\left[\kappa_1\left(\sum_{\ell=0}^{\infty}P^{\ell}E_{\ell}(\varkappa)\right)-(\vartheta+\kappa_2)\left(\sum_{\ell=0}^{\infty}P^{\ell}I_{\ell}(\varkappa)\right)\right]d\varkappa, \tag{75}$$

$$\begin{aligned}\sum_{\ell=0}^{\infty}P^{\ell}C_{\ell}(\xi)&=C(0)+\frac{p}{\Gamma\varsigma}\int_0^{\xi}(\xi-\varkappa)^{\varsigma-1}\left[\vartheta q_1\left(\sum_{\ell=0}^{\infty}P^{\ell}C_{\ell}(\varkappa)\right)+q_3\kappa_2\left(\sum_{\ell=0}^{\infty}P^{\ell}I_{\ell}(\varkappa)\right)\right.\\&\quad\left.-(\vartheta+\kappa_3)\left(\sum_{\ell=0}^{\infty}P^{\ell}C_{\ell}(\varkappa)\right)-\rho_2\left(\sum_{\ell=0}^{\infty}P^{\ell}C_{\ell}(\varkappa)\right)\right]d\varkappa,\end{aligned} \tag{76}$$

$$\begin{aligned}\sum_{\ell=0}^{\infty}P^{\ell}R_{\ell}(\xi)&=R(0)+\frac{p}{\Gamma\varsigma}\int_0^{\xi}(\xi-\varkappa)^{\varsigma-1}\left[\vartheta q_2\left(\sum_{\ell=0}^{\infty}P^{\ell}R_{\ell}(\varkappa)\right)-(\vartheta+\kappa_4)\left(\sum_{\ell=0}^{\infty}P^{\ell}C_{\ell}(\varkappa)\right)\right.\\&\quad\left.-\rho_1\left(\sum_{\ell=0}^{\infty}P^{\ell}S_{\ell}(\varkappa)\right)+\kappa_3\left(\sum_{\ell=0}^{\infty}P^{\ell}C_{\ell}(\varkappa)\right)+\rho_2\left(\sum_{\ell=0}^{\infty}P^{\ell}C_{\ell}(\varkappa)\right)\right.\end{aligned}$$

$$+(1-q_3)\,\kappa_2\left(\sum_{\ell=0}^{\infty}P^{\ell}I_{\ell}(\varkappa)\right)\Bigg]\,d\varkappa. \tag{77}$$

Computing the coefficient of distinct powers of p to both sides, we obtain

$$p^0 : S_0(\xi) = S(0), \quad S(0) = S_0, \tag{78}$$
$$p^0 : E_0(\xi) = E(0) \quad E(0) = E_0, \tag{79}$$
$$p^0 : I_0(\xi) = I(0), \quad I(0) = I_0, \tag{80}$$
$$p^0 : C_0(\xi) = C(0), \quad C(0) = C_0, \tag{81}$$
$$p^0 : R_0(\xi) = R(0), \quad R(0) = R_0. \tag{82}$$

Also,

$$\begin{aligned} p^1 : S_1(\xi) = \frac{1}{\Gamma\varsigma}\int_0^{\xi}(\xi-\varkappa)^{\varsigma-1}\,[\vartheta - \vartheta q_1 C_0(\varkappa) - \vartheta q_2 R_0(\varkappa) - q'(I_0(\varkappa)S_0(\varkappa)) \\ -q'\mu(C_0(\varkappa)S_0(\varkappa)) - \vartheta S_0(\varkappa) - \rho_1 S_0(\varkappa) + \kappa_4 R_0(\varkappa)]\,d\varkappa, \end{aligned} \tag{83}$$

$$\begin{aligned} p^1 : E_1(\xi) = \frac{1}{\Gamma\varsigma}\int_0^{\xi}(\xi-\varkappa)^{\varsigma-1}\,[q'(I_0(\varkappa)S_0(\varkappa)) + q'\mu(C_0(\varkappa)S_0(\varkappa)) \\ -(\vartheta+\kappa_1)E_0(\varkappa)]\,d\varkappa, \end{aligned} \tag{84}$$

$$p^1 : I_1(\xi) = \frac{1}{\Gamma\varsigma}\int_0^{\xi}(\xi-\varkappa)^{\varsigma-1}\,[\kappa_1 E_0(\varkappa) - (\vartheta+\kappa_2)I_0(\varkappa)]\,d\varkappa, \tag{85}$$

$$\begin{aligned} p^1 : C_1(\xi) = \frac{1}{\Gamma\varsigma}\int_0^{\xi}(\xi-\varkappa)^{\varsigma-1}\,[\vartheta q_1(C_0(\varkappa)) + q_3\kappa_2(I_0(\varkappa)) \\ -(\vartheta+\kappa_3)C_0(\varkappa) - \rho_2 C_0(\varkappa)]\,d\varkappa, \end{aligned} \tag{86}$$

$$\begin{aligned} p^1 : R_1(\xi) = \frac{1}{\Gamma\varsigma}\int_0^{\xi}(\xi-\varkappa)^{\varsigma-1}\,[\vartheta q_2(R_0(\varkappa)) + (1-q_3)\kappa_2(I_0(\varkappa)) + \kappa_3(C_0(\varkappa)) \\ -\vartheta(R_0(\varkappa)) - \kappa_4(R_0(\varkappa)) + \rho_1(S_0(\varkappa)) + \rho_2 C_0(\varkappa)]\,d\varkappa. \end{aligned} \tag{87}$$

Similarly, we get

$$\begin{aligned} p^2 : S_2(\xi) = \frac{1}{\Gamma\varsigma}\int_0^{\xi}(\xi-\varkappa)^{\varsigma-1}\,[\vartheta - \vartheta q_1(C_1(\varkappa)) - \vartheta q_2(R_1(\varkappa)) \\ -q'(I_0(\varkappa)S_1(\varkappa)) - q'\mu(I_1(\varkappa)S_0(\varkappa)) - q'\mu(C_0(\varkappa)S_1(\varkappa)) \\ -q'(C_1(\varkappa)S_0(\varkappa)) - \vartheta(S_1(\varkappa)) - \rho_1(S_1(\varkappa)) + \kappa_4(R_1(\varkappa))]\,d\varkappa, \end{aligned} \tag{88}$$

$$p^2 : E_2(\xi) = \frac{1}{\Gamma\varsigma}\int_0^{\xi}(\xi-\varkappa)^{\varsigma-1}\,[q'(I_0(\varkappa)S_1(\varkappa)) + q'(I_1(\varkappa)S_0(\varkappa))$$

$$+q'\mu\left(C_0\left(\varkappa\right)S_1\left(\varkappa\right)\right)+q'\mu\left(C_1\left(\varkappa\right)S_0\left(\varkappa\right)\right)-\left(\vartheta+\kappa_1\right)E_1\left(\varkappa\right)\big]\,d\varkappa, \tag{89}$$

$$p^2: I_2\left(\xi\right)=\frac{1}{\Gamma\varsigma}\int_0^{\xi}\left(\xi-\varkappa\right)^{\varsigma-1}\left[\kappa_1E_1\left(\varkappa\right)-\left(\vartheta+\kappa_2\right)I_1\left(\varkappa\right)\right]d\varkappa, \tag{90}$$

$$\begin{aligned}p^2: C_2\left(\xi\right)=\frac{1}{\Gamma\varsigma}\int_0^{\xi}\left(\xi-\varkappa\right)^{\varsigma-1}&\left[\vartheta q_1\left(C_1\left(\varkappa\right)\right)+q_3\kappa_2\left(I_1\left(\varkappa\right)\right)\right.\\&\left.-\left(\vartheta+\kappa_3\right)C_1\left(\varkappa\right)-\rho_2C_1\left(\varkappa\right)\right]d\varkappa,\end{aligned} \tag{91}$$

$$\begin{aligned}p^2: R_2\left(\xi\right)=\frac{1}{\Gamma\varsigma}\int_0^{\xi}\left(\xi-\varkappa\right)^{\varsigma-1}&\left[\vartheta q_2\left(R_1\left(\varkappa\right)\right)+\left(1-q_3\right)\kappa_2\left(I_1\left(\varkappa\right)\right)+\kappa_3\left(C_1\left(\varkappa\right)\right)\right.\\&\left.-\vartheta\left(R_1\left(\varkappa\right)\right)-\kappa_4\left(R_1\left(\varkappa\right)\right)+\rho_1\left(S_1\left(\varkappa\right)\right)+\rho_2\left(C_1\left(\varkappa\right)\right)\right]d\varkappa.\end{aligned} \tag{92}$$

.
.
.

$$\begin{aligned}p^{\ell}: S_{\ell}\left(\xi\right)=\frac{1}{\Gamma\varsigma}\int_0^{\xi}\left(\xi-\varkappa\right)^{\varsigma-1}&\left[\vartheta-\vartheta q_1\left(C_{\ell-1}\left(\varkappa\right)\right)-\vartheta q_2\left(R_{\ell-1}\left(\varkappa\right)\right)\right.\\&-q'\sum_{j=0}^{\ell-1}\left(I_j\left(\varkappa\right)S_{\ell-j-1}\left(\varkappa\right)\right)-q'\mu\sum_{j=0}^{\ell-1}\left(C_j\left(\varkappa\right)S_{\ell-j-1}\left(\varkappa\right)\right)\\&\left.-\vartheta\left(S_{\ell-1}\left(\varkappa\right)\right)-\rho_1\left(S_{\ell-1}\left(\varkappa\right)\right)+\kappa_4\left(R_{\ell-1}\left(\varkappa\right)\right)\right]d\varkappa,\end{aligned} \tag{93}$$

$$\begin{aligned}p^{\ell}: E_{\ell}\left(\xi\right)=\frac{1}{\Gamma\varsigma}\int_0^{\xi}\left(\xi-\varkappa\right)^{\varsigma-1}&\left[q'\sum_{j=0}^{\ell-1}\left(I_j\left(\varkappa\right)S_{\ell-j-1}\left(\varkappa\right)\right)+q'\mu\sum_{j=0}^{\ell-1}\left(C_j\left(\varkappa\right)S_{\ell-j-1}\left(\varkappa\right)\right)\right.\\&\left.-\left(\vartheta+\kappa_1\right)E_{\ell-1}\left(\varkappa\right)\right]d\varkappa,\end{aligned} \tag{94}$$

$$p^{\ell}: I_{\ell}\left(\xi\right)=\frac{1}{\Gamma\varsigma}\int_0^{\xi}\left(\xi-\varkappa\right)^{\varsigma-1}\left[\kappa_1E_{\ell-1}\left(\varkappa\right)-\left(\vartheta+\kappa_2\right)I_{\ell-1}\left(\varkappa\right)\right]d\varkappa, \tag{95}$$

$$\begin{aligned}p^{\ell}: C_{\ell}\left(\xi\right)=\frac{1}{\Gamma\varsigma}\int_0^{\xi}\left(\xi-\varkappa\right)^{\varsigma-1}&\left[\vartheta q_1\left(C_{\ell-1}\left(\varkappa\right)\right)+q_3\kappa_2\left(I_{\ell-1}\left(\varkappa\right)\right)\right.\\&\left.-\left(\vartheta+\kappa_3\right)C_{\ell-1}\left(\varkappa\right)-\rho_2C_{\ell-1}\left(\varkappa\right)\right]d\varkappa,\end{aligned} \tag{96}$$

$$\begin{aligned}p^{\ell}: R_{\ell}\left(\xi\right)=\frac{1}{\Gamma\varsigma}\int_0^{\xi}\left(\xi-\varkappa\right)^{\varsigma-1}&\left[\vartheta q_2\left(R_{\ell-1}\left(\varkappa\right)\right)+\left(1-q_3\right)\kappa_2\left(I_{\ell-1}\left(\varkappa\right)\right)+\kappa_3\left(C_{\ell-1}\left(\varkappa\right)\right)\right.\\&\left.-\vartheta\left(R_{\ell-1}\left(\varkappa\right)\right)-\kappa_4\left(R_{\ell-1}\left(\varkappa\right)\right)+\rho_1\left(S_{\ell-1}\left(\varkappa\right)\right)+\rho_2\left(C_{\ell-1}\left(\varkappa\right)\right)\right]d\varkappa.\end{aligned} \tag{97}$$

Hence, the series solution of the proposed HBV model is given as

$$S(\xi) = S_0 + S_1(\xi) + S_2(\xi) + \cdots, \tag{98}$$
$$E(\xi) = E_0 + E_1(\xi) + E_2(\xi) + \cdots, \tag{99}$$
$$I(\xi) = I_0 + I_1(\xi) + I_2(\xi) + \cdots, \tag{100}$$
$$C(\xi) = C_0 + C_1(\xi) + C_2(\xi) + \cdots, \tag{101}$$
$$R(\xi) = R_0 + R_1(\xi) + R_2(\xi) + \cdots. \tag{102}$$

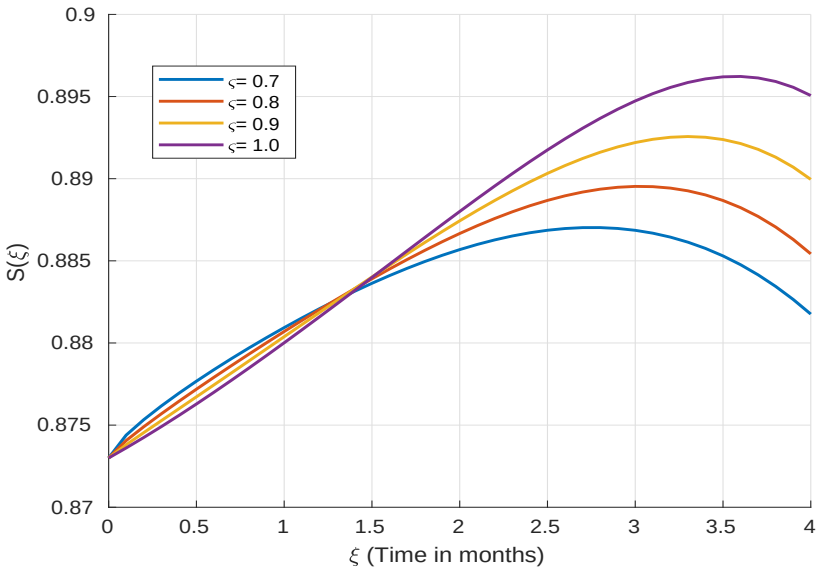

Figure 1: Graphical nature of susceptible individuals $S(\xi)$with respect to ξ at different order of ς

6 Numerical solution

In this section, we present the numerical simulations to illustrate the dynamical behavior of the proposed fractional-order HBV model and to validate the analytical results obtained via the homotopy decomposition method. The simulations are carried out using MATLAB for both fractional-order $(0 < \varsigma < 1)$ and classical integer-order $(\varsigma = 1)$ cases. The parameter values are adopted from [24] and are fixed throughout the simulations as $q_1 = 0.11$, $q_2 = 0.10$, $q_3 = 0.059$, $\vartheta = 0.0121$, $q' = 0.820$, $\mu = 0.1$, $\kappa_1 = 6$, $\kappa_2 = 4$, $\kappa_3 = 0.025$, and $\kappa_4 = 0.06$. The initial conditions are chosen to be biologically meaningful and consistent with earlier studies.

Figure 1 shows the temporal variation of the susceptible population $S(\xi)$ for different values of the fractional order ς. It is observed that the susceptible population decreases over time for all values of ς, which is consistent with the continuous recruitment of individuals into the exposed class through effective contact with infected and carrier individuals. Moreover, the rate of decline depends on the

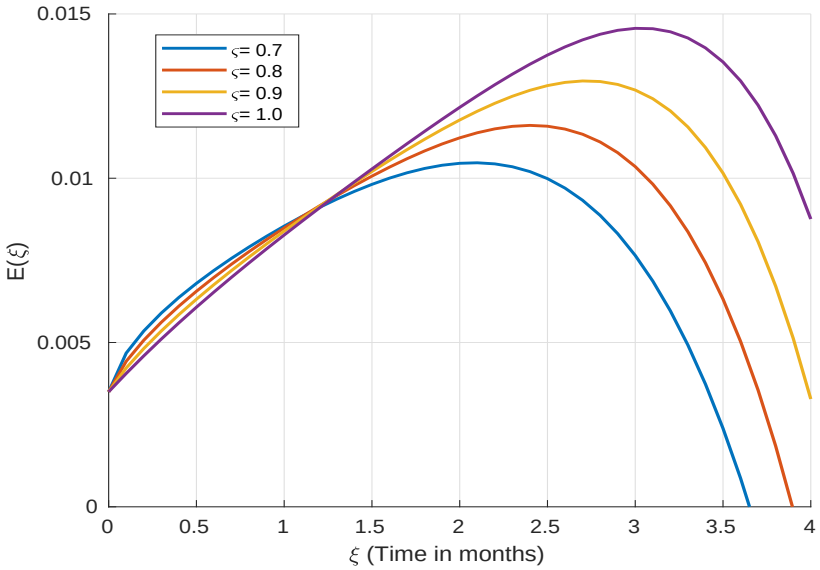

Figure 2: Graphical nature of infected exposed $E(\xi)$ with respect to ξ at different order of ς

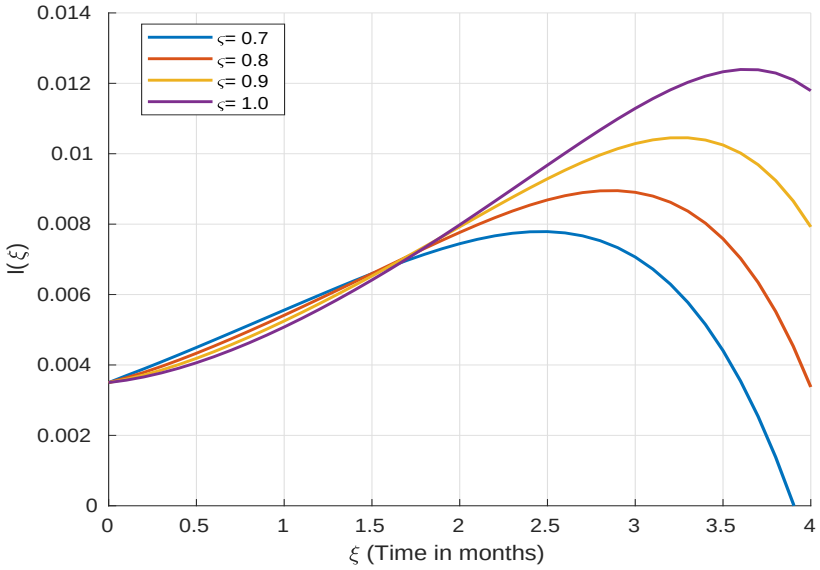

Figure 3: Graphical nature of infected individuals $I(\xi)$ with respect to ξ at different order of ς

fractional order, with lower values of ς leading to a relatively faster reduction. This behavior reflects the influence of memory effects embedded in the fractional-order operator, which modifies the rate at which susceptible individuals respond to the cumulative infection pressure.

Figure 2 and Figure 3 illustrate the dynamics of the exposed population $E(\xi)$ and the infected population $I(\xi)$ respectively. A clear distinction is observed between the fractional-order cases ($\varsigma =$

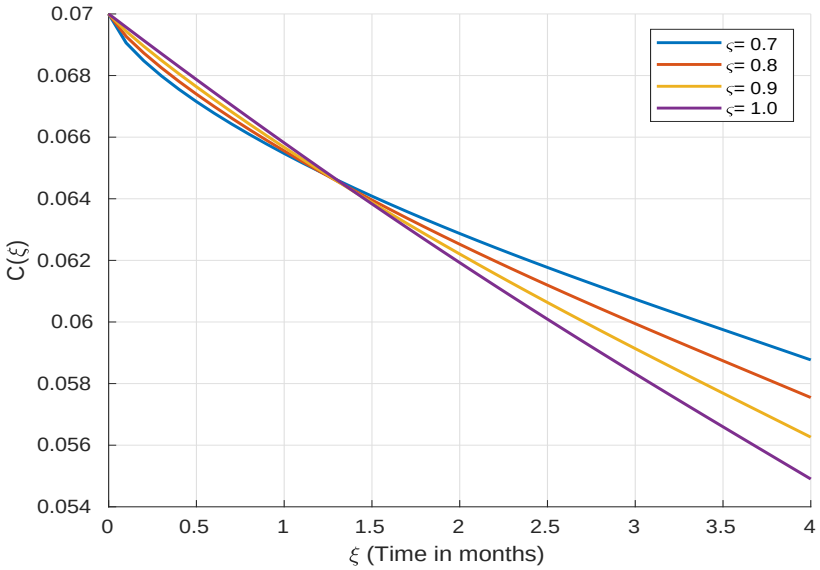

Figure 4: Graphical nature of chronic individuals $C(\xi)$ with respect to ξ at different order of ς

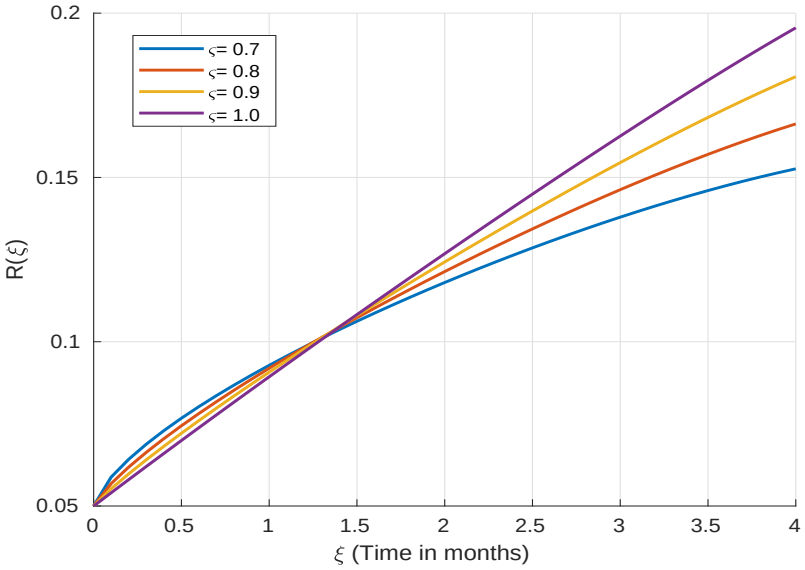

Figure 5: Graphical nature of recovered individuals $R(\xi)$ with respect to ξ at different order of ς

$0.7, 0.8, 0.9$) and the classical integer-order model ($\varsigma = 1.0$). For $\varsigma = 1.0$, both $E(\xi)$ and $I(\xi)$ decay gradually, corresponding to a memoryless evolution of the disease dynamics. In contrast, the fractional-order solutions exhibit a faster decline, and the deviation from the classical case becomes more pronounced as ς decreases. Among the fractional cases, $\varsigma = 0.9$ shows a moderate reduction compared to the integer-order model, while $\varsigma = 0.8$ and $\varsigma = 0.7$ result in a significantly steeper decrease. This compar-

ison highlights the magnitude of the effect introduced by the fractional-order memory and demonstrates that the classical model may overestimate the persistence of exposed and infected individuals. From a modeling perspective, the accelerated decay of $E(\xi)$ and $I(\xi)$ at lower fractional orders can be attributed to the nonlocal nature of the Caputo fractional derivative, which incorporates the cumulative history of the disease into the present dynamics. Lower values of ς correspond to weaker persistence of past infection states, leading to a more rapid attenuation of these compartments. Epidemiologically, this behavior suggests that the fractional-order formulation provides a more flexible framework for capturing delayed responses and long-term effects of intervention strategies such as vaccination and treatment.

Figure 4 depicts the temporal evolution of the chronic carrier population $C(\xi)$ for different fractional orders. The results show a monotonic decrease in the carrier population over time with fractional-order cases exhibiting a faster reduction compared to the integer-order model. This trend is consistent with the combined effects of treatment and recovery parameters, as well as the reduced inflow from the infected class due to the accelerated decay of $I(\xi)$ under fractional dynamics. The influence of the fractional order is again evident, as lower values of ς lead to a more pronounced decline in chronic carriers. Finally, Figure 5 presents the dynamics of the recovered population $R(\xi)$. It is observed that $R(\xi)$ increases over time for all values of ς, reflecting the cumulative effect of recovery from infected and carrier classes. The fractional-order solutions show a slightly faster growth compared to the classical case, particularly for smaller values of ς. This behavior is consistent with the reduced persistence of infection and carrier states in the fractional-order model.

7 Conclusions

In this paper, we constructed criteria for studying the HBV model from both qualitative and analytical perspectives, demonstrating the existence and solution of the proposed model using the Banach theorem. To explore the transmission and vaccination process of HBV in greater depth. We developed an algorithm to obtain approximate solutions and presented graphical results that illustrate the dynamics of the model. The analysis of susceptible, exposed, infected, chronic carriers, and recovered populations under both integer-order and fractional-order cases shows that vaccination significantly reduces infection prevalence, and lower fractional orders accelerate this decline by capturing memory effects in disease progression. The main outcomes of this study reveal that vaccination is highly effective in reducing HBV spread, recovery improves with treatment, and chronic carrier density can be minimized through vaccination strategies. Moreover, the fractional-order model provides a more realistic and biologically meaningful representation of HBV dynamics compared to classical models. Overall, the findings confirm that the proposed technique is effective for studying complex biological models, and the S–E–I–C–R formulation addresses a real-life health problem by quantifying the long-term benefits of preventive measures in high-prevalence populations, which is consistent with international experiences in hepatitis B control.

Declarations

Conflict of interest

There is no conflict of interests regarding the publication of this paper.

Funding

There is no funding regarding the publication of this paper.

Acknowledgment

The author thanks the referees and editor for the positive and constructive comments, which helped improve the manuscript.

Data availability statement

All data that support the findings of this study are included within the article.

Using of AI tools:

The authors declare that they have not used Artificial Intelligence (AI) tools in the creation of this article.

References

[1] R. Agarwal, S.D. Purohit, Kritika, *A mathematical fractional model with nonsingular kernel for thrombin receptor activation in calcium signalling*, Math. Methods Appl. Sci. **42** (2019) 7160–7171.

[2] R. Agarwal, Kritika, S.D. Purohit, J. Mishra, *A mathematical fractional model to study the hepatitis B virus infection*, Mathematical Modeling and Soft Computing in Epidemiology, CRC Press (2020) 273–290.

[3] G. Ajileye, O.O. Aduroja, T.P. Pantuvo, A.M. Ayinde, *A numerical method for solving non-linear Volterra integro-differential equation of fractional order*, Math. Comput. Sci. **4** (2024) 17–25.

[4] A. Ali, K. Shah, R.A. Khan, *Numerical treatment for traveling wave solutions of fractional Whitham–Broer–Kaup equations*, Alex. Eng. J. **57** (2018) 1991–1998.

[5] S.S. Alzaid, B.S.T. Alkahtani, S. Sharma, R.S. Dubey, *Numerical solution of fractional model of HIV-1 infection in framework of different fractional derivatives*, J. Funct. Spaces **2021** (2021) 6642957.

[6] R.M. Anderson, R.M. May, *Infectious Diseases of Humans: Dynamics and Control*, Oxford Univ. Press (1991).

[7] F. Arif, Z. Majeed, J.U. Rahman, N. Iqbal, J. Kafle, *Mathematical modeling and numerical simulation of the outbreak of COVID-19 involving loss of immunity and quarantined class*, Comput. Math. Methods Med. **2022** (2022) 1–21.

[8] R. Arora, D. Kumar, I. Jhamb, A.K. Narang, *Mathematical modeling of Chikungunya dynamics: Stability and simulation*, Cubo (Temuco) **22** (2020) 177–201.

[9] A. Atangana, E. Alabaraoye, *Solving a system of fractional partial differential equations arising in the model of HIV infection of CD4+ cells and attractor one-dimensional Keller–Segel equations*, Adv. Differ. Equ. **2013** (2013) 94.

[10] B. Babayar-Razlighi, *Numerical solution of an influenza model with vaccination and antiviral treatment by the Newton-Chebyshev polynomial method*, J. Math. Model. **11** (2023) 103-116.

[11] E. Bonyah, Z. Hammouch, M.E. Koksal, *Mathematical modeling of coronavirus dynamics with conformable derivative in Liouville–Caputo sense*, J. Math. **2022** (2022) Article ID 8353343.

[12] E. Demirci, A. Unal, N. Ozalp, *A fractional order SEIR model with density dependent death rate*, Hacet. J. Math. Stat. **40** (2011) 287–295.

[13] Fatmawati, M.A. Khan, E. Bonyah, Z. Hammouch, E.M. Shaiful, *A mathematical model of tuberculosis (TB) transmission with children and adults groups: A fractional model*, AIMS Math. **5** (2020) 2813–2842.

[14] W. Gao, P. Veeresha, H.M. Baskonus, D.G. Prakasha, P. Kumar, *A new study of unreported cases of 2019-nCOV epidemic outbreaks*, Chaos Solit. Fractals **138** (2020) 109929.

[15] M.M. Gour, L.K. Yadav, S.D. Purohit, D.L. Suthar, *Homotopy decomposition method to analyze fractional hepatitis B virus infection model*, Appl. Math. Sci. Eng. **31** (2023) 2260075.

[16] V. Gulkaç, *An extrapolation method for oxygen diffusion problem*, Int. J. Sci. Eng. Res. **6** (2015) 222–226.

[17] V. Gulkaç, *Comparative study between two numerical methods for oxygen diffusion problem*, Commun. Numer. Methods Eng. **25** (2009) 855–863.

[18] H. Habenom, D.L. Suthar, D. Baleanu, S.D. Purohit, *A numerical simulation on the effect of vaccination and treatments for the fractional hepatitis B model*, J. Comput. Nonlinear Dyn. **16** (2021) 011004.

[19] Z. Hammouch, R.R.Q. Rasul, A. Elazzouzi, *Mathematical analysis and numerical simulation of the Ebola epidemic disease in the sense of conformable derivative*, Chaos Solit. Fractals **158** (2022) 112006.

[20] A.A. Hamou, R.R.Q. Rasul, Z. Hammouch, N. Özdemir, *Analysis and dynamics of a mathematical model to predict unreported cases of COVID-19 epidemic in Morocco*, Comput. Appl. Math. **41** (2022) 289.

[21] F. Haq, K. Shah, G. ur Rahman, M. Shahzad, *Numerical solution of fractional order smoking model via Laplace Adomian decomposition method*, Alex. Eng. J. **57** (2018) 1061–1069.

[22] N. Iqbal, Y. Karaca, *Pattern formation induced by fractional-order diffusive model of COVID-19*, Multi-Chaos Fractal Multi-Fract. Artif. Intell. Complex Syst. (2022) 169–185.

[23] R. Jain, K. Arekar, R.S. Dubey, *Study of Bergman's minimal blood glucose-insulin model by Adomian decomposition method*, J. Inf. Optim. Sci. **38** (2017) 133–149.

[24] A.V. Kamyad, R. Akbari, A.A. Heydari, A. Heydari, *Mathematical modeling of transmission dynamics and optimal control of vaccination and treatment for hepatitis B virus*, Comput. Math. Methods Med. **2014** (2014) 1–15.

[25] R. Kaur, J. Prabhanshi, I. Jhamb, P. Verma, *Transmission dynamics of COVID-19 across a region: a mathematical model*, Proc. Natl. Acad. Sci. India Sect. A Phys. Sci. (2025) 1–16.

[26] S.A. Khan, K. Shah, G. Zaman, F. Jarad, *Existence theory and numerical solutions to smoking model under Caputo–Fabrizio fractional derivative*, Chaos **29** (2019) 013128.

[27] S.A. Khan, K. Shah, P. Kumam, A. Seadawy, G. Zaman, Z. Shah, *Study of mathematical model of Hepatitis B under Caputo–Fabrizio derivative*, AIMS Math. **6** (2021) 195–209.

[28] M.A. Khan, M. Alhaisoni, M. Nazir, A. Alqahtani, A. Binbusayyis, S. Alsubai, Y. Nam, B.G. Kang, *A healthcare system for COVID-19 classification using multi-type classical features selection*, Comput. Mater. Continua **74** (2023) 1–15.

[29] A. Khani, N. Belalzadeh, *Numerical solution of Volterra integral equations with weakly singular kernel using Legendre wavelet method*, Math. Comput. Sci. **6** (2025) 160–169.

[30] A.A. Kilbas, *Theory and Applications of Fractional Differential Equations*, North-Holland Math. Stud. **204** (2006).

[31] P. Kumar, M.P. Yadav, *Numerical approximations of groundwater flow problem using fractional variational iteration method with fractional derivative of singular and nonsingular kernels*, Int. J. Math. Ind. **16(1)** (2024) 2450008.

[32] M.L.G. Kuniyoshi, F.L.P.D. Santos, *Mathematical modelling of vector-borne diseases and insecticide resistance evolution*, J. Venom. Anim. Toxins Trop. Dis. **23** (2017) 34.

[33] W.M. Lee, *Hepatitis B virus infection*, N. Engl. J. Med. **337** (1997) 1733–1745.

[34] S.R. Lewin, R.M. Ribeiro, T. Walters, G.K. Lau, S. Bowden, S. Locarnini, A.S. Perelson, *Analysis of hepatitis B viral load decline under potent therapy: complex decay profiles observed*, Hepatology **34** (2001) 1012–1020.

[35] A.C. Loyinmi, A.L. Ijaola, *Investigating the effects of some control measures on the dynamics of diphtheria infection using fractional order model*, Math. Comput. Sci. **5** (2024) 26–47.

[36] J. Mann, M. Roberts, *Modelling the epidemiology of hepatitis B in New Zealand*, J. Theor. Biol. **269** (2011) 266–272.

[37] G.F. Medley, N.A. Lindop, W.J. Edmunds, D.J. Nokes, *Hepatitis-B virus endemicity: heterogeneity, catastrophic dynamics and control*, Nat. Med. **7** (2001) 619–624.

[38] J.A. Nanaware, A.L. Dongardive, *Double ARA-Sumudu decomposition method for the solution of linear fractional partial integro-differential equations*, Math. Comput. Sci. **6** (2025) 102–111.

[39] N. Negero, G. Duressa, *An efficient numerical approach for singularly perturbed parabolic convection-diffusion problems with large time-lag*, J. Math. Model. **10** (2022) 173-190.

[40] M.A. Nowak, S. Bonhoeffer, A.M. Hill, R. Boehme, H.C. Thomas, H. McDade, *Viral dynamics in hepatitis B virus infection*, Proc. Natl. Acad. Sci. **93** (1996) 4398–4402.

[41] I. Podlubny, *Fractional Differential Equations*, Math. Sci. Eng., Elsevier **198** (1999).

[42] S.M. Salman, A.M. Yousef, *On a fractional-order model for HBV infection with cure of infected cells*, J. Egypt. Math. Soc. **25** (2017) 445–451.

[43] A.B. Saqib, G. Barid Loghmani, M. Heydari, *Convergence analysis of compact finite difference method for the solution of anti-periodic boundary value problems*, J. Math. Model. **12** (2024) 1-15.

[44] M. Shrahili, R.S. Dubey, A. Shafay, *Inclusion of fading memory to Banister model of changes in physical condition*, Discret. Contin. Dyn. Syst. Ser. S **13** (2020) 881–888.

[45] S. Thornley, C. Bullen, M. Roberts, *Hepatitis B in a high prevalence New Zealand population: a mathematical model applied to infection control policy*, J. Theor. Biol. **254** (2008) 599–603.

[46] C. Vargas-De-Leon, *Stability analysis of a model for HBV infection with cure of infected cells and intracellular delay*, Appl. Math. Comput. **219** (2012) 389–398.

[47] K. Wang, W. Wang, S. Song, *Dynamics of an HBV model with diffusion and delay*, J. Theor. Biol. **253** (2008) 36–44.

[48] WHO, *Hepatitis B Fact Sheet No. 204*, World Health Organization, Geneva, Switzerland (2013).

[49] M.P. Yadav, R. Agarwal, S.D. Purohit, D. Kumar, D.L. Suthar, *Groundwater flow in karstic aquifer: analytic solution of dual-porosity fractional model to simulate groundwater flow*, Appl. Math. Sci. Eng. **30** (2022) 598–608.

[50] L.K. Yadav, G. Agarwal, M.M. Gour, M. Kumari, *Analytical approach to study weakly nonlocal fractional Schrödinger equation via novel transform*, Int. J. Dyn. Control **12** (2024) 271–282.

[51] S.K. Yadav, M. Purohit, M.M. Gour, L.K. Yadav, M.N. Mishra, *Hybrid technique for multi-dimensional fractional diffusion problems involving Caputo–Fabrizio derivative*, Int. J. Math. Ind. **16(1)** (2024) 2450020.

[52] L.K. Yadav, M.M. Gour, V.K. Meena, E. Bonyah, S.D. Purohit, *Approximate analytical solutions of fractional coupled Whitham–Broer–Kaup equations via novel transform*, Int. J. Optim. Control Theor. Appl. **15** (2025) 35–49.

[53] H. Ye, Y. Ding, *Nonlinear dynamics and chaos in a fractional-order HIV model*, Math. Probl. Eng. **2009** (2009) 78614.

[54] S.J. Zhao, Z.Y. Xu, Y. Lu, *A mathematical model of hepatitis B virus transmission and its application for vaccination strategy in China*, Int. J. Epidemiol. **29** (2000) 744–752.